



Article

Overexpressing Carotenoid Biosynthetic Genes in *Synechocystis* sp. PCC 6803 Improved Intracellular Pigments and Antioxidant Activity, Which Can Decrease the Viability and Proliferation of Lung Cancer Cells In Vitro

Maturin Natesungnoen ¹, Varisa Pongrakhananon ² , Peter Lindblad ³ and Saowarath Jantaro ^{1,*}

¹ Laboratory of Cyanobacterial Biotechnology, Department of Biochemistry, Faculty of Science, Chulalongkorn University, Bangkok 10330, Thailand

² Department of Pharmacology and Physiology, Faculty of Pharmaceutical Sciences, Chulalongkorn University, Bangkok 10330, Thailand

³ Microbial Chemistry, Department of Chemistry—Ångström, Uppsala University, P.O. Box 523, SE-75120 Uppsala, Sweden

* Correspondence: saowarath.j@chula.ac.th; Tel.: +66-2-218-5431; Fax: +66-2-218-5418

Abstract: In the antioxidant system in cyanobacteria, non-enzymatic antioxidants, such as carotenoids, are considered good candidates for coping with oxidative stress, particularly light stress, and pharmaceutical therapeutic applications. A significant amount of carotenoid accumulation has been recently improved by genetic engineering. In this study, to achieve higher carotenoid production with higher antioxidant activity, we successfully constructed five *Synechocystis* sp. PCC 6803 strains overexpressing (OX) native genes related to the carotenoids biosynthetic pathway, including OX_CrtB, OX_CrtP, OX_CrtQ, OX_CrtO, and OX_CrtR. All of the engineered strains maintained a significant quantity of myxoxanthophyll, while increasing zeaxanthin and echinenone accumulation. In addition, higher components of zeaxanthin and echinenone were noted in all OX strains, ranging from 14 to 19% and from 17 to 22%, respectively. It is worth noting that the enhanced echinenone component responded to low light conditions, while the increased β -carotene component contributed to a high light stress response. According to the higher antioxidant activity of all OX strains, the carotenoid extracts presented lower IC₅₀ in lung cancer cell lines H460 and A549, with values less than 157 and 139 μ g/mL, respectively, when compared with those of WTc, particularly OX_CrtR and OX_CrtQ. A higher proportion of zeaxanthin and β -carotene in OX_CrtR and OX_CrtQ, respectively, may considerably contribute to the ability to treat lung cancer cells with antiproliferative and cytotoxic effects.

Keywords: carotenoids; *Synechocystis* sp. PCC 6803; lung cancer cells; antioxidant activity



Citation: Natesungnoen, M.; Pongrakhananon, V.; Lindblad, P.; Jantaro, S. Overexpressing Carotenoid Biosynthetic Genes in *Synechocystis* sp. PCC 6803 Improved Intracellular Pigments and Antioxidant Activity, Which Can Decrease the Viability and Proliferation of Lung Cancer Cells In Vitro. *Int. J. Mol. Sci.* **2023**, *24*, 9370. <https://doi.org/10.3390/ijms24119370>

Academic Editor: Francesco Caruso

Received: 4 May 2023

Revised: 21 May 2023

Accepted: 23 May 2023

Published: 27 May 2023



Copyright: © 2023 by the authors. Licensee MDPI, Basel, Switzerland. This article is an open access article distributed under the terms and conditions of the Creative Commons Attribution (CC BY) license (<https://creativecommons.org/licenses/by/4.0/>).

1. Introduction

Carotenoids (Cars), present in all oxygenic photoautotrophic organisms, are intracellular pigments that are typically encased in cellular membranes and assist in the assembly and function of photosynthetic complexes [1–5]. Carotenes and their oxygenated derivatives, i.e., xanthophylls such as echinenone, myxoxanthophyll, nostoxanthine, and zeaxanthin, belong to a group of Cars. Their functions serve as not only accessory light-harvesting pigments but also as photoprotective agents when cells are exposed to light stress, such as high light intensity and ultraviolet radiation [6–8]. Regarding the hydrophobic molecules of β -carotene and echinenone, they are able to form complexes with proteins, thereby functioning as a bridge between proteins in photosynthetic systems [1,5], as well as a scavenger of singlet oxygen [9–11]. The xanthophylls were found to have a stronger scavenging character than the carotenes [12]. Although there is currently no evidence that the xanthophylls bind to membrane proteins, it was expected that xanthophylls would rigidify membranes,

while β -carotene and echinenone probably have a fluidizing impact [2]. In photosynthesis, Cars can act as antioxidants, detoxifying harmful reactive oxygen species (ROS); accept the excess energy from photosensitized molecules such as chlorophyll or singlet oxygen; and form a triplet state before being released it as heat to the ground state [12]. In terms of human health and disease treatment, dietary Cars or foods rich in Cars are considered beneficial in preventing severe diseases such as cancer, psoriasis, cardiovascular diseases, neurodegenerative disorders, and ocular disorders [13–16]. Cars have a certain influence on diminishing the oncogenic progress by, for instance, controlling oxidative stress, apoptosis, cell cycle progression, and metastasis [16–18]. In addition, Cars serve as antioxidants in normal cells, while they act as pro-oxidants in cancer cells by interacting with lipid peroxy radicals to form the Car radical cation (Cars \bullet), resulting in a higher ROS level with higher damage to cellular biomolecules [16,19,20].

In Figure 1, the Car biosynthetic pathway in the cyanobacterium *Synechocystis* sp. PCC 6803 starts from the condensation of geranylgeranyl pyrophosphate (GGPP, 2 molecules) to generate 15-cis-phytoene via a phytoene synthase (CrtB, EC 2.5.1.32, encoded by the *slr1255* gene). Phytoene is then converted to respective ζ -carotene and lycopene via phytoene desaturase (CrtP, EC 1.3.5.5, encoded by the *slr1254* gene), and ζ -carotene desaturase (CrtQ, EC 1.3.5.6, encoded by *slr0940* gene). Although the genes encoding the lycopene epsilon cyclase and lycopene beta cyclase (EC 5.5.1.19) responsible for the cyclization reaction of lycopene to γ -carotene and β -carotene, respectively, have been predicted in some cyanobacteria as CrtL-type, such as *P9211_07411*(epsilon)/*P9211_11261*(beta) of *Prochlorococcus marinus* str. MIT 9211, *sync_0974*(beta) of *Synechococcus* sp. CC9311, and CruP and CruA of *Synechococcus* sp. PCC7002 [21], it has not yet been identified in *Synechocystis* strains in the Cyanobase database (<https://genome.microbedb.jp>, accessed on 28 April 2023). However, the *Sll0254* gene encoding bifunctional lycopene cyclase/dioxygenase (CrtL^{diox}) in *Synechocystis* sp. PCC 6803 was previously considered to be required in myxoxanthophyll biosynthesis, but there has not yet been experimental evidence on its catalyzing β -carotene production [22]. Then, a β -carotene intermediate is converted to echinenone using the β -carotene ketolase (CrtO, EC 1.14.99.63, encoded by the *slr0088* gene). The localization levels of CrtQ and CrtO enzymes are abundantly located in plasma membranes, as compared to in thylakoid membranes [1]. Subsequently, β -carotene hydroxylase (CrtR, EC 1.14.13.129, encoded by the *sll1468* gene) effectively converts β -carotene to zeaxanthin, as well as myxoxanthophyll and 3'-hydroxyechinenone syntheses [1,23,24]. On the other hand, the connected biosynthetic pathways between carotenoids and chlorophyll occur at the GGPP intermediate which can be converted to phytyl-PP by geranylgeranyl reductase (ChlP, EC 1.3.1.83, encoded by the *sll1091* gene) [25]. In addition, chlorophyll synthase (ChlG, EC 2.5.1.62, encoded by the *slr0056* gene) catalyzed the last reaction of chlorophyll synthesis by esterifying chlorophyllide with phytyl-PP. For chlorophyll degradation, although there is still no gene encoding chlorophyllase retrieved in *Synechocystis* sp. PCC 6803, the phytol kinase (EC 2.7.1.182) encoded by the *slr1652* gene is found to catalyze the conversion of phytol to phytol monophosphate (phytol-P). Meanwhile, the degradation of carotenoids occurs via non-specific mechanisms, such as oxidation, and generates β -apo-carotenal, which is further converted to retinal using the Dio1 or ACO enzyme (EC 1.14.99.36, encoded by the *sll1541* gene) [26,27].

In this study, we improved total Cars and Car components with higher antioxidant activity by constructing five engineered *Synechocystis* sp. PCC6803 strains with overexpressing genes involved in the carotenoid biosynthetic pathway (Figure 1). Five engineered strains consisted of (1) *Synechocystis* sp. PCC6803, overexpressing the *slr1255* gene or OX_CrtB, (2) *Synechocystis* sp. PCC6803, overexpressing the *slr1254* gene or OX_CrtP, (3) *Synechocystis* sp. PCC6803, overexpressing the *slr0940* gene or OX_CrtQ, (4) *Synechocystis* sp. PCC6803, overexpressing the *slr0088* gene or OX_CrtO, and (5) *Synechocystis* sp. PCC6803, overexpressing the *sll1468* gene or OX_CrtR. In addition, all engineered strains contained a significant increase in total lipids when compared to the wild-type control. Particularly, the cell viability and proliferation of H460 and A549 lung cancer cell lines

could be markedly reduced by carotenoid extracts from OX strains when compared to the wild-type control.

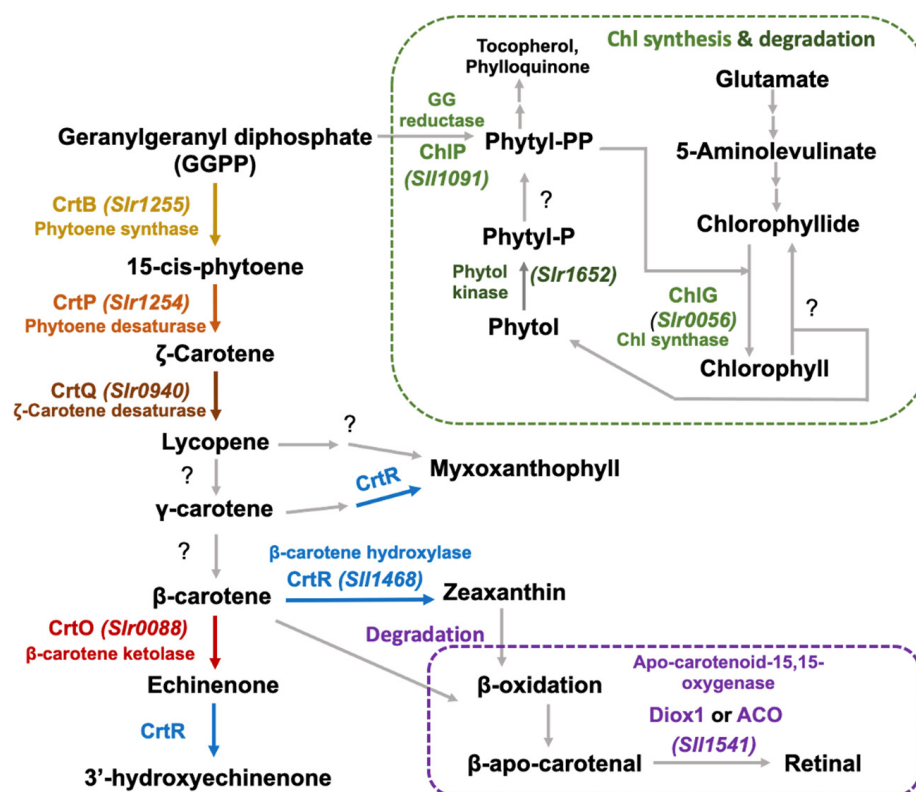


Figure 1. A tentative scheme of carotenoid synthesis and degradation in relation to chlorophyll synthesis and degradation (modified from [1,25,27]). Genes encoding enzymes in each pathway are indicated in italics. The scheme indicates “?” representing enzymes that are encoded by unidentified genes in *Synechocystis* sp. PCC 6803.

2. Results

2.1. *Synechocystis* sp. PCC 6803 Mutant Strains and Their Carotenoid Contents under Normal Growth Conditions

Six engineered *Synechocystis* sp. PCC 6803 strains, including the wild-type control (WTc), OX_CrtB, OX_CrtP, OX_CrtQ, OX_CrtO, and OX_CrtR (Table 1), were constructed via a double homologous recombination. The wild-type control (WTc) strain was generated by substituting the *psbA2* gene with a *Cm^R* cassette (Figure 2A), whereas each OX strain was created by substituting the *psbA2* gene with each gene fragment in the *Synechocystis* wild-type (WT) genome (Figure 2A–E). The complete segregation in *Synechocystis* genome was confirmed by PCR using Uppsba2 and DSpsba2 primers (B Primers, Figure 2 and Supplementary Information Table S1). In the WTc strain, PCR products using B Primers showed no band, while it showed a 2.4 kb gene fragment when using A Primers. In Figure 2A–E, PCR products with the A Primers of OX_CrtB, OX_CrtP, OX_CrtQ, OX_CrtO, and OX_CrtR strains confirmed the correct sizes of 2.2, 2.5, 2.6, 2.7, and 2.0 kb, respectively, whereas PCR products with B Primers confirmed the correct sizes of 3.4, 3.7, 3.7, 3.9, and 3.2 kb, respectively.

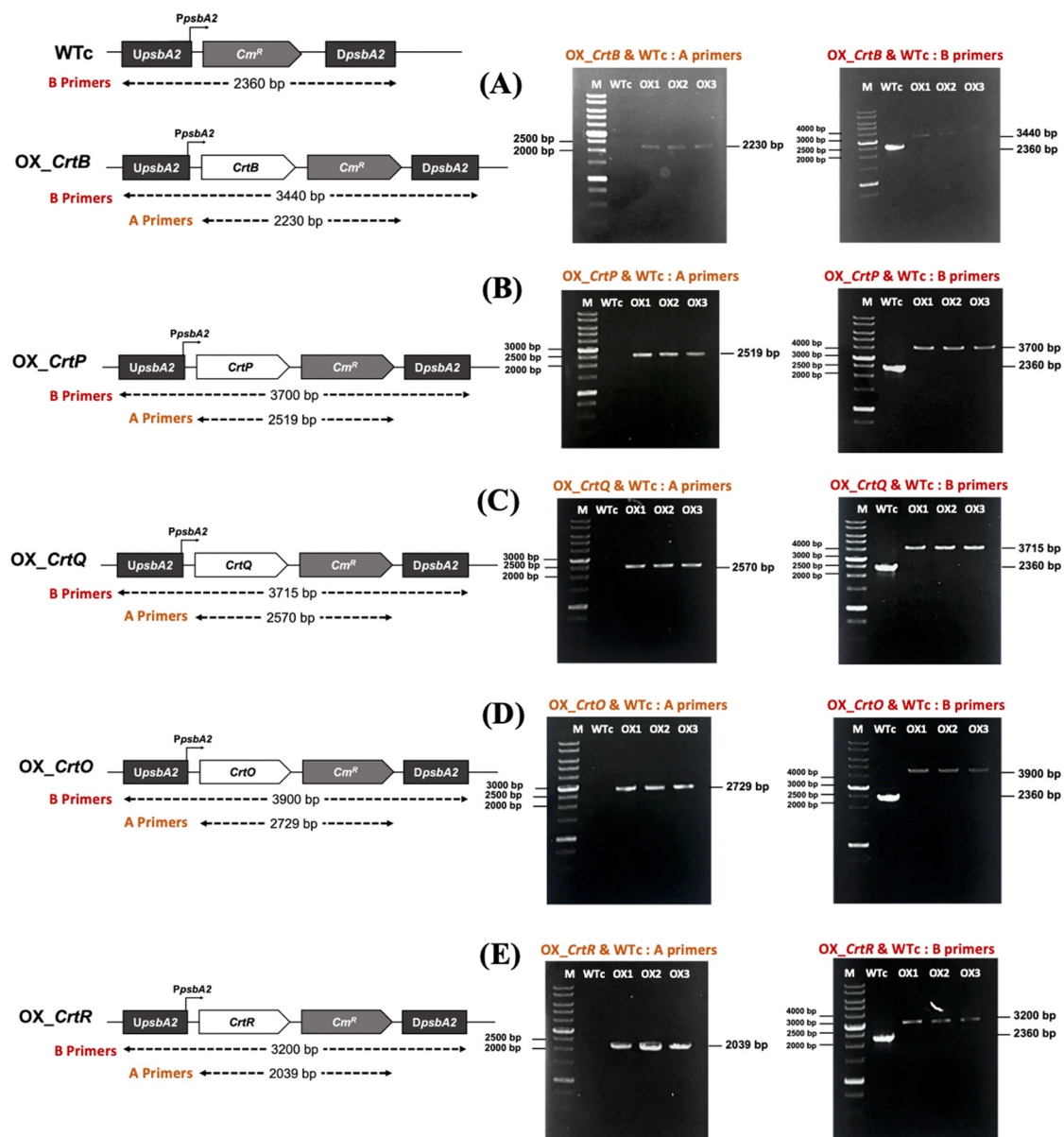


Figure 2. Genomic maps of engineered *Synechocystis* sp. PCC 6803 strains, including OX_CrtB (A), OX_CrtP (B), OX_CrtQ (C), OX_CrtO (D), and OX_CrtR (E). The specific primers (Supplementary information Table S1) were chosen to confirm the integration of each gene into the *Synechocystis* genome. All strains were constructed by overexpressing each native gene in the wild-type control. The confirmation of integration was verified by PCR with genomic DNA from WT and engineered strains as the template. The A Primers comprise a forward primer of a gene and a reverse primer of *Cm^R*, while the B Primers are UpsbA2 and DpsbA2 primers. Lane M: GeneRuler DNA ladder (Fermentas). For (A) for OX_CrtB, the A Primers were FW_CrtB and RV_Cm^R; Lane 1: WTc, Lanes 2–4: clone numbers 1–3 (OX1, OX2, OX3). For (B) for OX_CrtP, the A Primers were FW_CrtP and RV_Cm^R; Lane 1: WTc, Lanes 2–4: clone numbers 1–3 (OX1, OX2, and OX3). For (C) for OX_CrtQ, the A Primers were FW_CrtQ and RV_Cm^R; Lane 1: WTc, Lanes 2–4: clone numbers 1–3 (OX1, OX2, and OX3). For (D) for OX_CrtO, the A Primers were FW_CrtO and RV_Cm^R; Lane 1: WTc, Lanes 2–4: clone numbers 1–3 (OX1, OX2, and OX3). For (E) for OX_CrtR, the A Primers were FW_CrtR and RV_Cm^R; Lane 1: WTc, Lanes 2–4: clone numbers 1–3 (OX1, OX2, and OX3).

Table 1. Strains and plasmids used in this study.

Name	Relevant Genotype	Reference
Cyanobacterial strains		
<i>Synechocystis</i> sp. PCC 6803	Wild type	Pasteur Culture Collection
Wild-type control (WTc)	<i>Cm^R</i> integrated at the region of a native <i>psbA2</i> gene in the <i>Synechocystis</i> genome	This study
OX_ <i>CrtB</i>	<i>CrtB</i> and <i>Cm^R</i> integrated at the region of a native <i>psbA2</i> gene in the <i>Synechocystis</i> genome	This study
OX_ <i>CrtP</i>	<i>CrtP</i> and <i>Cm^R</i> integrated at the region of a native <i>psbA2</i> gene in the <i>Synechocystis</i> genome	This study
OX_ <i>CrtQ</i>	<i>CrtQ</i> and <i>Cm^R</i> integrated at the region of a native <i>psbA2</i> gene in the <i>Synechocystis</i> genome	This study
OX_ <i>CrtO</i>	<i>CrtO</i> and <i>Cm^R</i> integrated at the region of a native <i>psbA2</i> gene in the <i>Synechocystis</i> genome	This study
OX_ <i>CrtR</i>	<i>CrtR</i> and <i>Cm^R</i> integrated at the region of a native <i>psbA2</i> gene in the <i>Synechocystis</i> genome	This study
Plasmids		
pEERM	P _{psbA2} - <i>Cm^R</i> ; plasmid containing the flanking region of a <i>psbA2</i> gene	This study
pEERM_ <i>CrtB</i>	P _{psbA2} - <i>CrtB</i> ; integrated between the <i>PstI</i> sites of pEERM	This study
pEERM_ <i>CrtP</i>	P _{psbA2} - <i>CrtP</i> ; integrated between the <i>XbaI</i> and <i>SpeI</i> sites of pEERM	This study
pEERM_ <i>CrtQ</i>	P _{psbA2} - <i>CrtQ</i> ; integrated between the <i>XbaI</i> and <i>SpeI</i> sites of pEERM	This study
pEERM_ <i>CrtO</i>	P _{psbA2} - <i>CrtO</i> ; integrated between the <i>SpeI</i> and <i>PstI</i> sites of pEERM	This study
pEERM_ <i>CrtR</i>	P _{psbA2} - <i>CrtR</i> ; integrated between the <i>SpeI</i> and <i>PstI</i> sites of pEERM	This study

P_{psbA2}, strong *psbA2* promoter; *Cm^R*, chloramphenicol resistance cassette.

In addition, RT-PCR data verified the gene overexpression in all OX strains with a higher transcript amount in comparison with those of WTc (Figure 3A). For total carotenoid content, the increased carotenoid accumulation in OX strains was noted when the cells were grown before reaching their late-log phase (12 days of cultivation) of growth under normal growth conditions (Figure 3B). At 12 days of growth, all OX strains cultivated under normal conditions had significantly increased contents of five Cars detected by HPLC, including myxoxanthophyll, zeaxanthin, 3'-hydroxy echinenone, echinenone, and β -carotene, with the exception of OX_*CrtQ*, OX_*CrtO*, and OX_*CrtR*, which had some reduced Car types (Figure 3C). The zeaxanthin and echinenone levels in all OX strains commonly increased by more than 1.2-fold as compared to WTc (Figure 3D). The results revealed that each component of the Car types was altered in the OX strains. OX_*CrtB* contained the increased amounts of all Car types, 1.1–1.3-fold that of WTc, except for 3'-hydroxyechinenone, whereas OX_*CrtP* contained the significant increases of all Car types, about 1.1–1.4-fold that of WTc, with the exception of β -carotene. For OX_*CrtQ*, the higher fold increase in each Car type was also observed, 1.2–1.3-fold that of WTc, except for myxoxanthophyll. Meanwhile, 3'-hydroxyechinenone and echinenone contents had a 1.6-fold increase compared with WTc, as noted in OX_*CrtO*. Interestingly, OX_*CrtR* had

substantial increases in all Car types except for β -carotene; zeaxanthin levels increased by 1.6-fold; and the contents of 3'-hydroxyechinenone and echinenone increased by 1.9- and 1.4-folds, respectively. Although we did not monitor protein levels or enzymatic activity, all OX strains notably showed the altered changes in each Car product in accordance with their biosynthetic pathway.

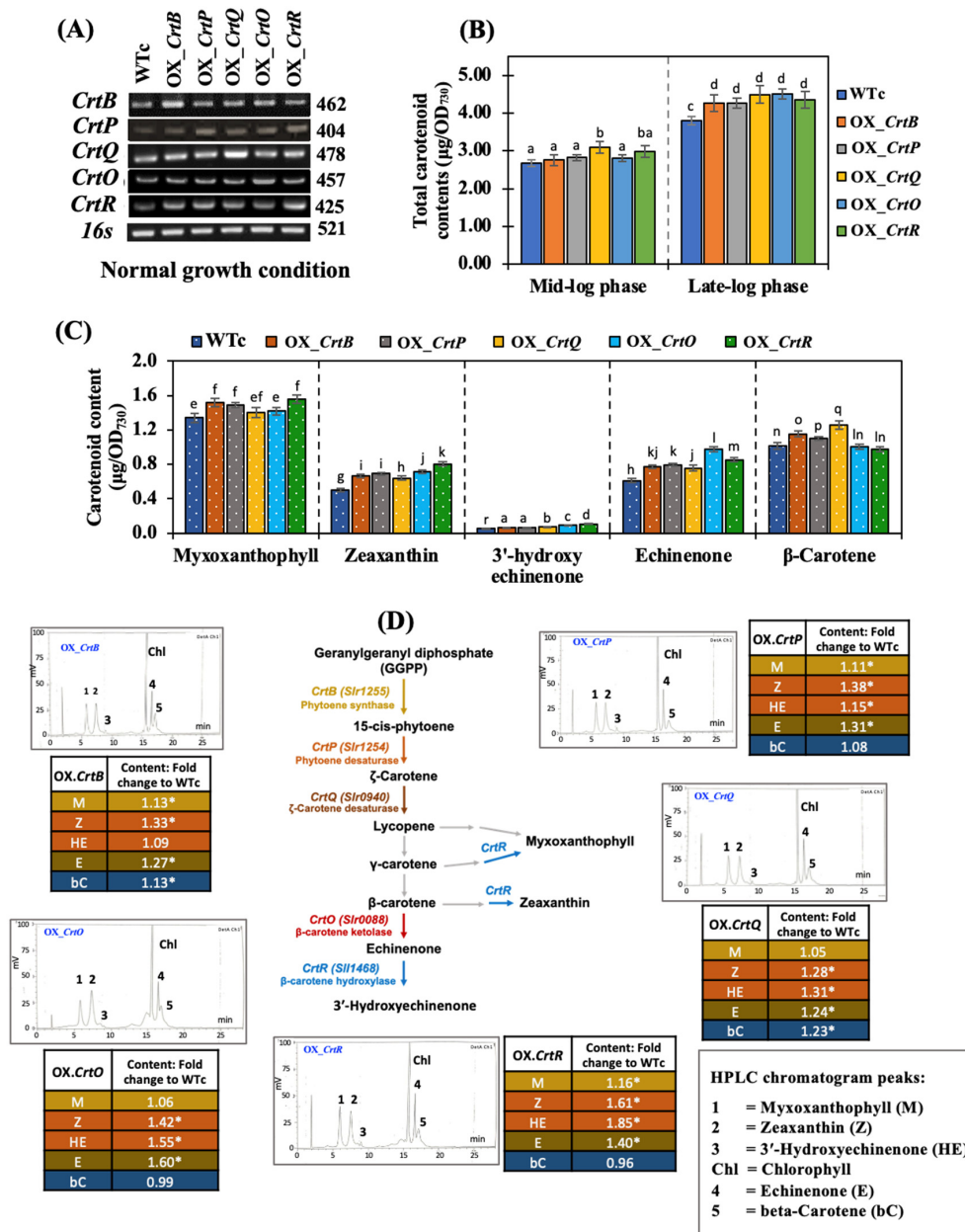


Figure 3. Transcript levels (A), total carotenoid contents (B), carotenoid contents (C), and fold changes of each content normalized with WTc and a HPLC chromatogram (D) of *Synechocystis* sp. PCC 6803 WTc and all engineered strains (OX). Cells were grown under normal growth conditions for 6 days (in (B)) and 12 days (A–C), representing the mid-log phase and late-log phases of cell growth, respectively. The error bars represent the standard deviations of means (mean \pm S.D., $n = 3$). Means with the same letters have nonsignificant differences at a significant level of $p < 0.05$. The statistical difference of the data between the values of WTc and the engineered strain is indicated by an asterisk at $* p < 0.05$. For (A), all cropped gels were taken from the original images of RT-PCR products on agarose gels, as shown in Supplementary Information Figure S2.

2.2. Growth and Intracellular Pigment Levels of Chlorophyll *a* and Carotenoids under Various Light Intensity Conditions

After exposing all strains to light stresses (Figure 4), low light (LL) conditions apparently affected the growth reduction in all strains, with the lowest growth rates found when comparing those of normal light (NL) and high light (HL) conditions. When cultivated under NL conditions, all OX strains only displayed a higher growth rate than WTc in the late-log phase (Figure 4A). However, they had great levels of growth than WTc under both LL and HL conditions throughout a 14-day treatment period (Figure 4B,C).

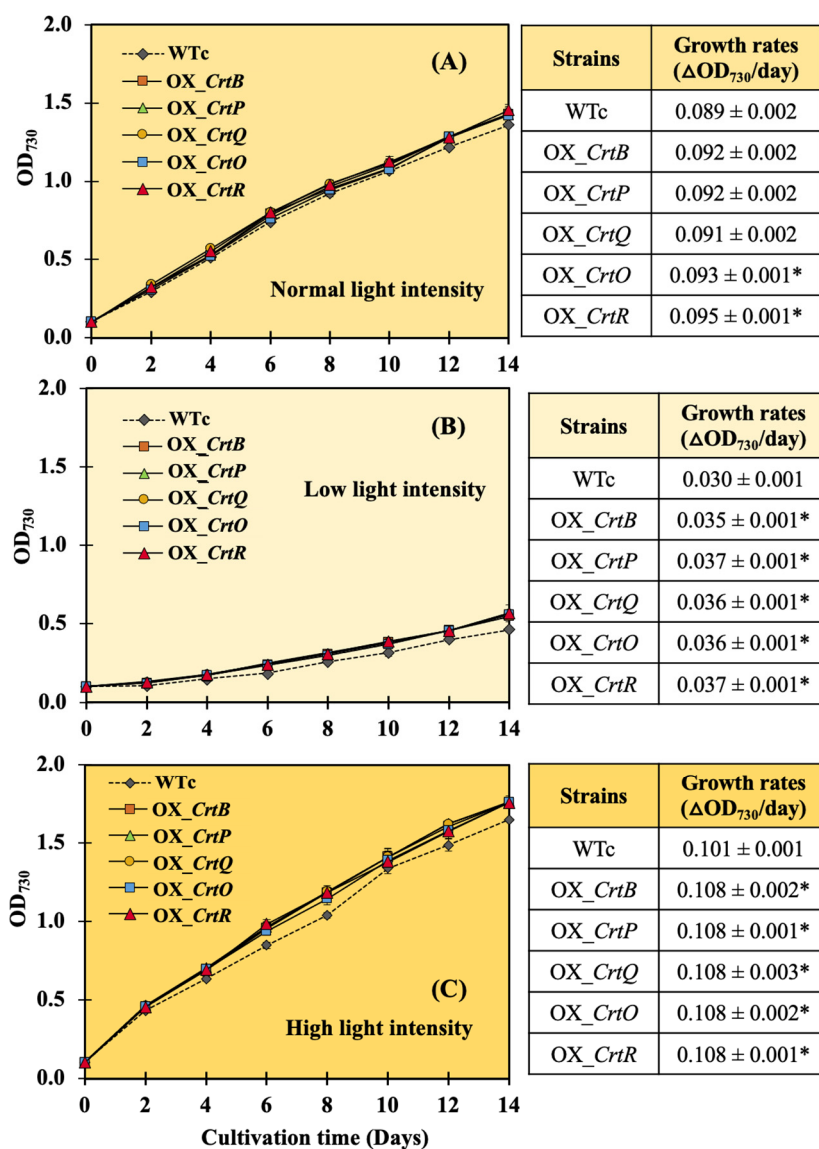


Figure 4. Growth curve and growth rates of *Synechocystis* sp. PCC6803 WTc and engineered strains grown in BG₁₁ medium under normal light (A), low light (B), and high light (C) conditions. The error bars represent standard deviations of means (mean \pm S.D., $n = 3$). The statistical difference of the data between the values of WTc and the engineered strain is indicated by an asterisk at $* p < 0.05$.

Intriguingly, all OX strains were promoted to accumulate more chlorophyll *a* than WTc (Figure 5). The HL condition resulted in more dark green cell cultures and a higher rise in chlorophyll *a* content than the NL condition after 6 days of treatment (Figure 5A,E). When compared to those under NL conditions, the LL condition undoubtedly lowered the chlorophyll *a* content and the lighter green types of cell culture after both 6 and 12 days

of treatment (Figure 5C). On the other hand, all OX strains had a considerable increase in total Car content, as anticipated under all light conditions (Figure 5B,D,F).

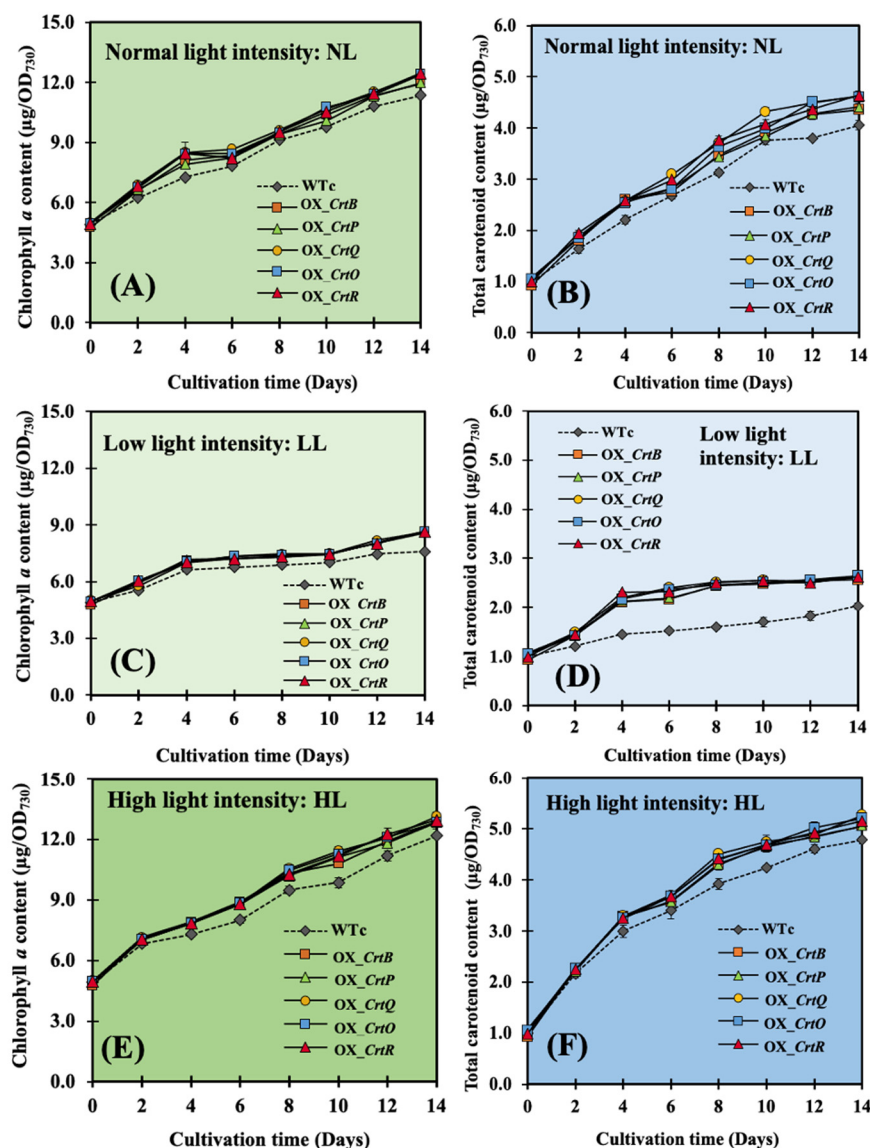


Figure 5. Chlorophyll (Chl) *a* (A,C,E) and total carotenoid (B,D,F) contents of *Synechocystis* sp. PCC6803 WTc and engineered strains. Cells were grown in BG₁₁ medium under normal light (A,B), low light (C,D), and high light (E,F) conditions. The error bars represent the standard deviations of means (mean \pm S.D., $n = 3$).

Six Car types, including myxoxanthophyll (M), zeaxanthin (Z), 3'-hydroxyechinenone (HE), echinenone (E), β -carotene (bC), and lycopene (L), of all strains were determined under LL and HL conditions (Figure 6). The increased Car accumulation of OX strains was significantly induced by LL and HL light stresses compared with those of WTc (Figure 6A–F). All *Synechocystis* strains apparently contained the highest amount of myxoxanthophyll, followed by β -carotene, echinenone, zeaxanthin, and other minor carotenoids (such as 3'-hydroxyechinenone and lycopene). Although lycopene was accumulated at relatively low levels, all OX strains showed a slight increase as compared to WTc (Figure 6F). This indicates that total Car accumulation was caused by HL stress rather than LL stress. Contrarily, under HL stress, β -carotene levels decreased in OX_CrtO and OX_CrtR, whereas they remained unaltered under NL conditions (Figure 6E).

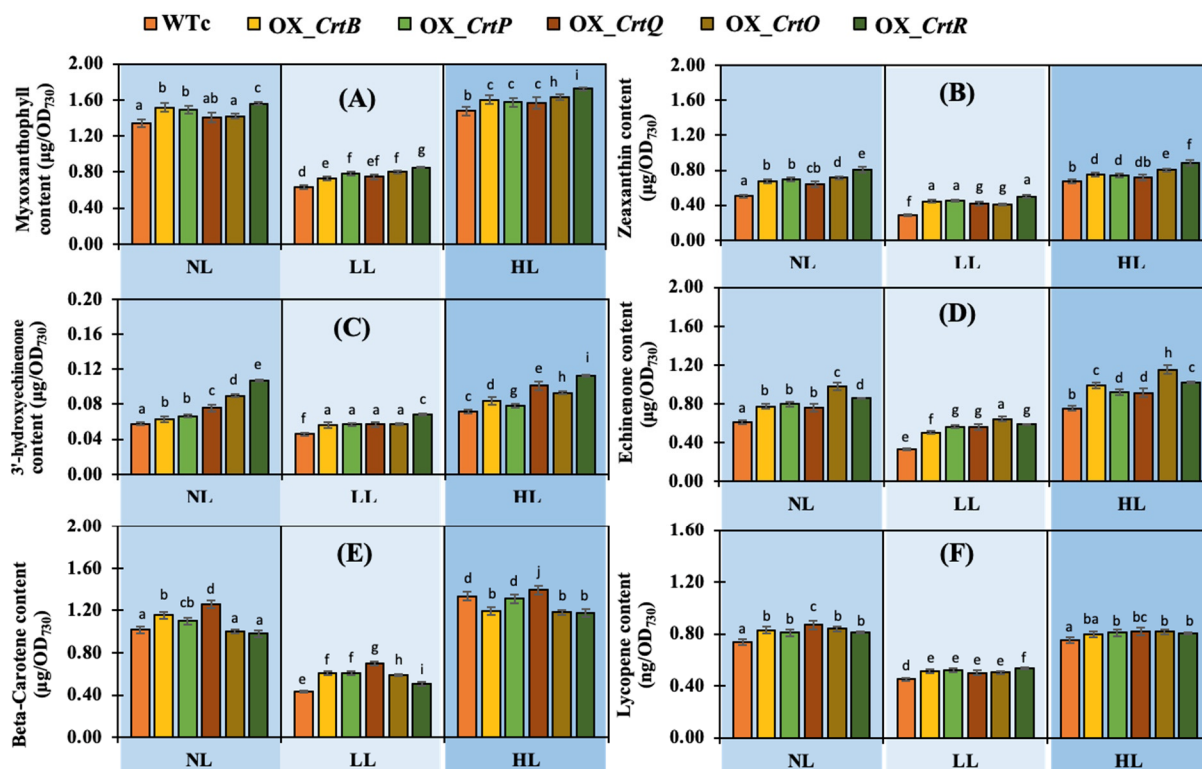


Figure 6. Carotenoid contents, including myxoxanthophyll (A), zeaxanthin (B), 3'-hydroxy echinenone (C), echinenone (D), β -carotene (E), and lycopene (F), of *Synechocystis* sp. PCC6803 WTc and engineered strains. Cells were grown in a BG₁₁ medium under normal light (NL), low light (LL), and high light (HL) conditions for 12 days (12 d). The error bars represent the standard deviations of means (mean \pm S.D., $n = 3$). Means with the same letters exhibit nonsignificant differences at a significant level of $p < 0.05$.

In addition, the relative percentage of each Car type was normalized with the total Car content (Figure 7A–C). Although myxoxanthophyll was mostly preserved as a main component in all *Synechocystis* cells, light stress caused cells to balance their Car component by slightly reducing the proportion of myxoxanthophyll. Under NL conditions, all OX strains had higher percentages of zeaxanthin and echinenone, approximately 14–19% and 17–22%, respectively, than WTc, with percentages of about 13 and 16%, respectively (Figure 7A). The HL condition at day 12 of treatment contained a similar pattern of carotenoid composition as those in the NL condition. On the other hand, stronger DPPH radical scavenging activity was shown in all OX strains than WTc under all light conditions (Figure 7D). The highest levels of antioxidant activity were found in the OX_CrtQ and OX_CrtR strains.

Additionally, the amounts of transcripts from genes involved in the biosynthesis and degradation of Cars and chlorophyll were monitored (Figure 8). The expression of genes involved in Car synthesis was substantially higher on day 12 of treatment under NL and HL conditions than that of genes involved in chlorophyll production and pigment degradation. In all strains cultivated under NL conditions, the transcript levels of the *CrtB* and *CrtQ* genes were the highest of all the genes involved in the Car synthetic pathway (Figure 8A). Furthermore, all five of the genes under investigation, particularly *CrtB* and *CrtR*, exhibited higher mRNA levels as a result of HL stress (Figure 8C). It is curiously interesting that OX strains had higher levels of *ChlG* and *ChlP* transcripts than WTc, in relation to chlorophyll synthesis, under all light conditions (Figure 8). In contrast, there was no difference in the transcript levels of *slr1652*, a gene involved in chlorophyll breakdown, and *Diox1*, a gene involved in Car degradation, under all light conditions.

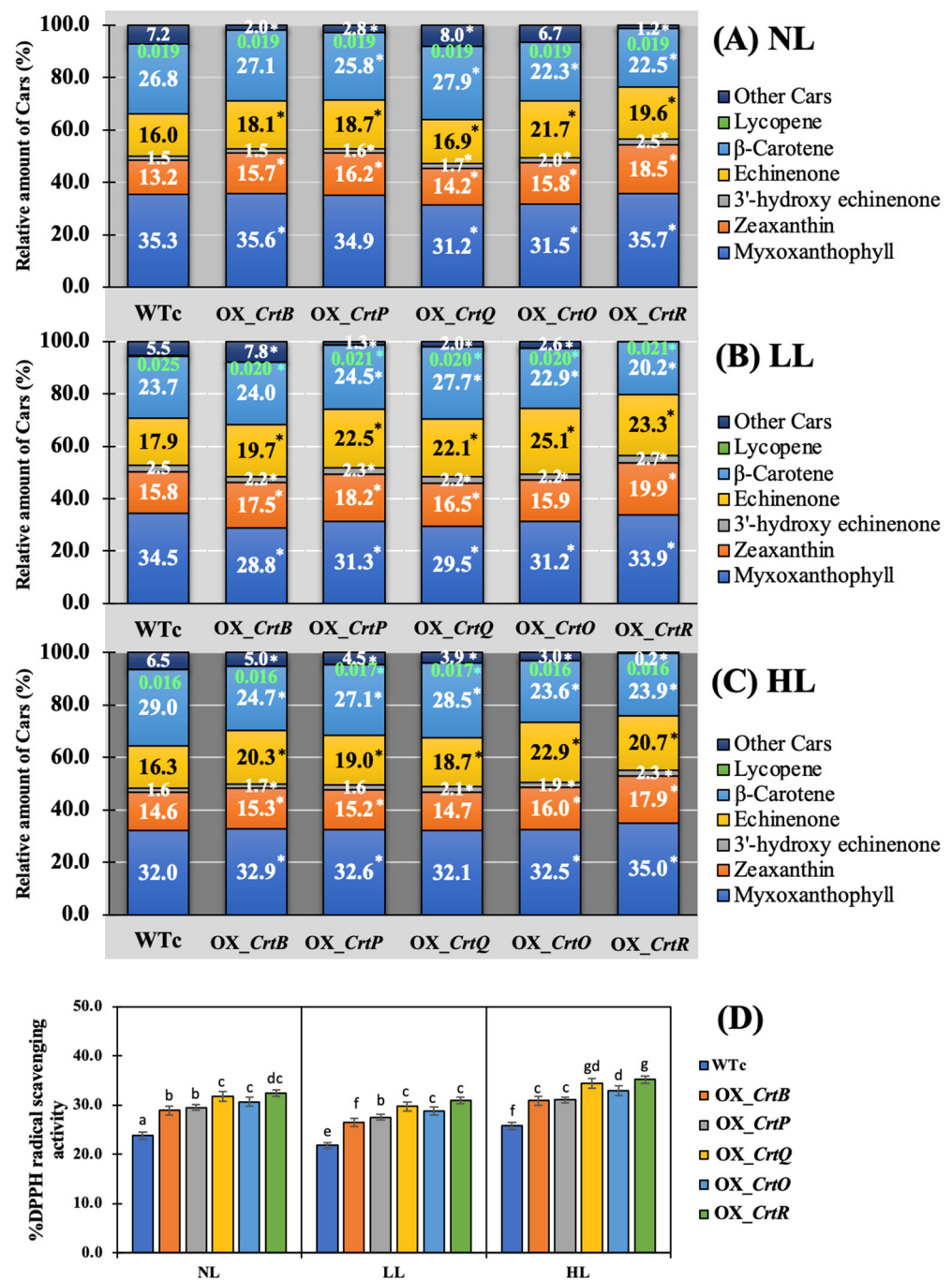


Figure 7. Percentage amounts of carotenoids (A–C) and %DPPH radical scavenging activities (D) of *Synechocystis* sp. PCC6803 WTc and engineered strains. Cells were grown in a BG₁₁ medium under (A) normal light (NL), (B) low light (LL), and (C) high light (HL) conditions for 12 days (12 d). The relative amount of Cars was calculated as a percentage relative to total carotenoid content under each light condition. For (A), the statistical difference of results between those values of WTc and that engineered strain under each condition is indicated by an asterisk at $p < 0.05$. For (D), the error bars represent the standard deviations of means (mean \pm S.D., $n = 3$). Means with the same letters have nonsignificant differences at a significant level of $p < 0.05$.

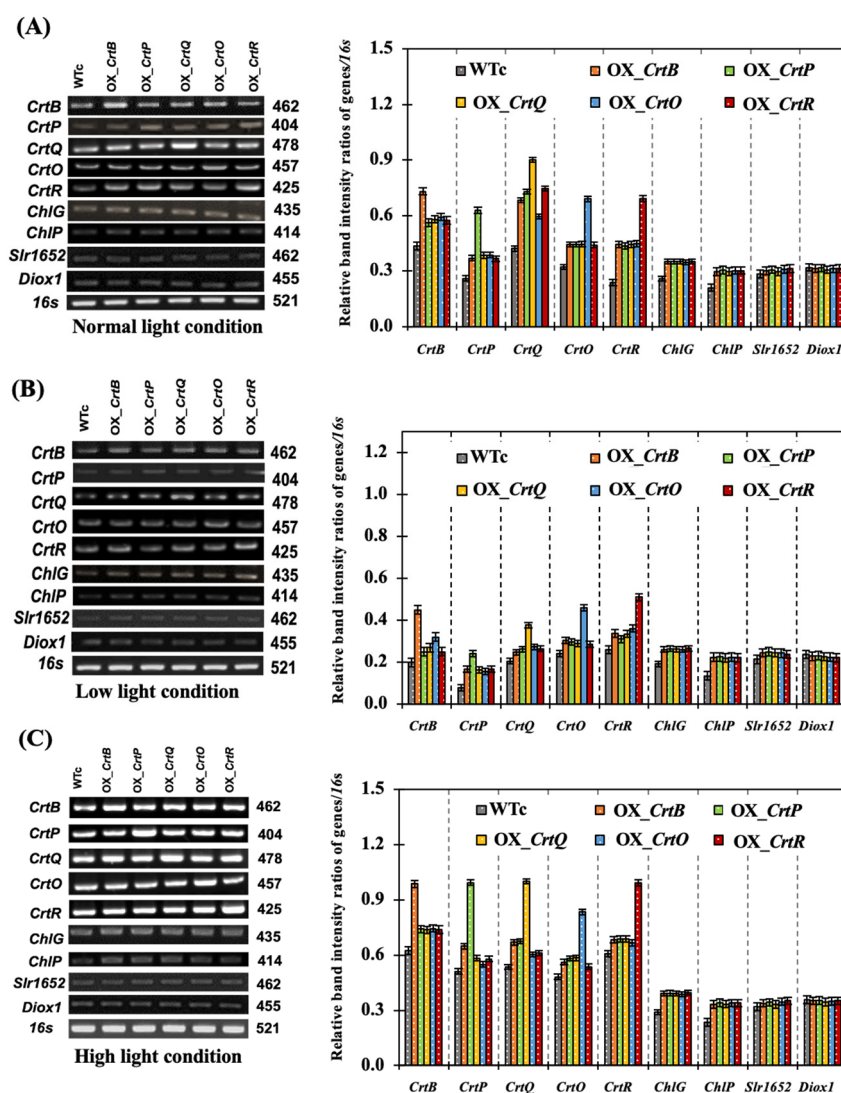


Figure 8. The transcript levels and relative intensity ratios of the *CrtB*, *CrtP*, *CrtQ*, *CrtO*, *CrtR*, *ChlG*, *ChlP*, *Slr1652*, *Diox1*, and *16s* rRNA genes of *Synechocystis* sp. PCC6803 WTc and engineered strains, grown in a BG₁₁ medium under normal light (A), low light (B), and high light (C) conditions for 12 days. The error bars represent the standard deviations of means (mean \pm S.D., n = 3). All cropped gels were taken from the original images of RT-PCR products on agarose gels, as shown in Supplementary Information Figures S2–S4.

2.3. Enhanced Intracellular Lipid Accumulation and Lung Cancer Cell Treatment

The cooperative function of lipids and Cars, particularly xanthophylls, has recently been found to stabilize the structure of the membrane and the photosystem in cyanobacteria [2,5,28]. In our study, all OX strains with a higher carotenoid content also had higher total lipid contents under all light conditions (Supplementary Information Figure S1). The HL condition at day 12 of treatment significantly increased the total lipid content when compared to the NL and LL conditions on the same day.

Extracted Cars from all strains were evaluated for their cytotoxicity and antiproliferative activities against two lung cancer cell lines (H460 and A549) (Figures 9 and 10). A half-maximal inhibitory concentration (IC₅₀) was determined in cancer cell lines (H460 and A549) to evaluate the cytotoxic effect of Car extracts at concentrations of 0–400 μ g/mL (Figure 9A,B). The results revealed that the IC₅₀ values for Car extracts from OX_CrtR, OX_CrtQ, OX_CrtO, OX_CrtB, and OX_CrtP in the H460 cell line, with values of 100.17 ± 2.27 , 113.46 ± 4.40 , 127.84 ± 4.16 , 137.57 ± 4.72 , and 137.54 ± 3.76 μ g/mL, respectively, were lower than those

of Car extracts from WTc ($157.60 \pm 6.48 \mu\text{g/mL}$) (Figure 9A). Furthermore, the IC_{50} values for Car extracts from OX_CrtR, OX_CrtQ, OX_CrtO, OX_CrtP, and OX_CrtB in the A549 cell line were lower than those of Car extracts from WTc ($139.79 \pm 7.29 \mu\text{g/mL}$), with values of 90.32 ± 2.13 , 100.99 ± 2.77 , 112.37 ± 3.45 , 126.44 ± 5.41 , and $124.83 \pm 5.95 \mu\text{g/mL}$, respectively (Figure 9B). Moreover, the relative cell proliferation level of lung cancer cell lines H460 and A549 after being treated with Car extracts for 72 h also decreased when compared with that of WTc (Figure 10A,B). The aberrant cancer cell lines with inhibited growth were discernible under a light microscope resulting from treatment with carotenoid extracts when compared to those of the control group without carotenoids (Figure 10C).

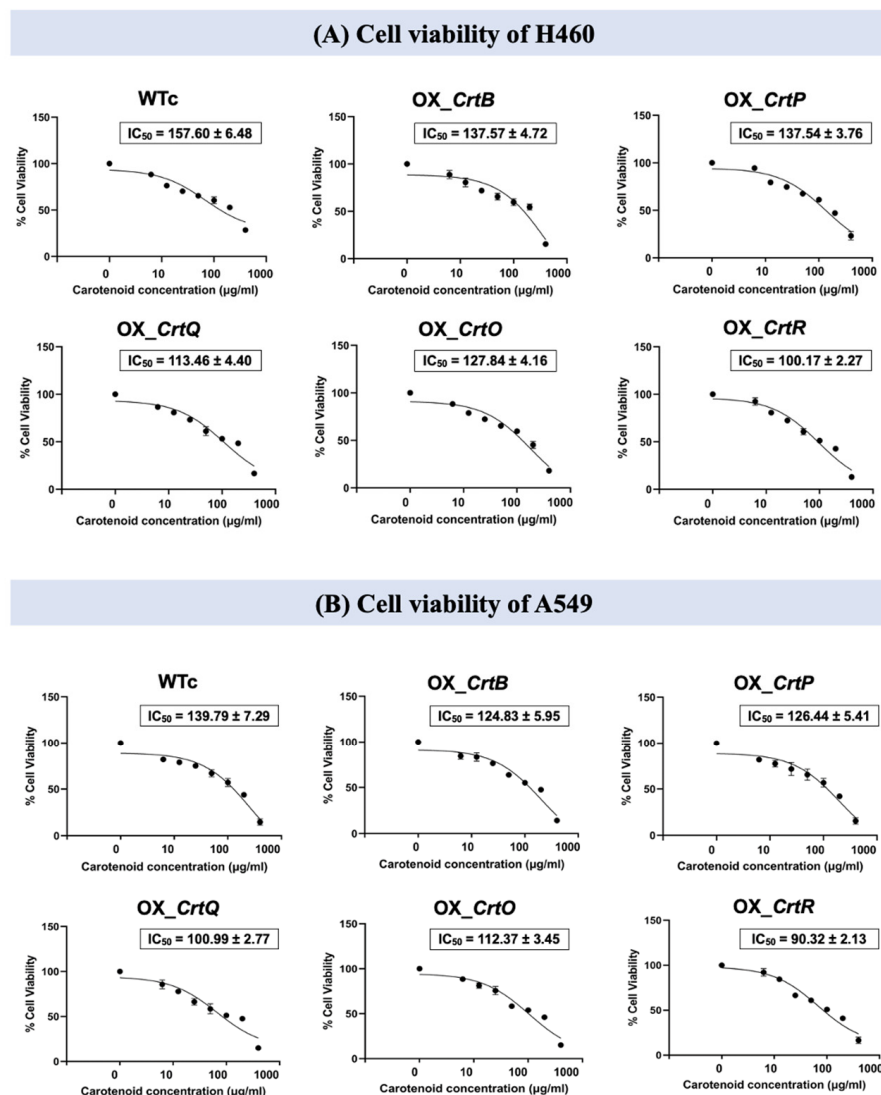


Figure 9. The IC_{50} values of cell viability in lung cancer cells H460 (A) and A549 (B) after being treated with total carotenoids extracted from *Synechocystis* sp. PCC6803 WTc and engineered strains. Total carotenoids were extracted from cells grown in a BG₁₁ medium under high light conditions for 12 days. Lung cancer cells were treated with various concentrations of carotenoid extracts (0–400 $\mu\text{g/mL}$, circles). The decreasing trendline of %cell viability was shown in black. The error bars represent standard deviations of means (mean \pm S.D., $n = 3$).

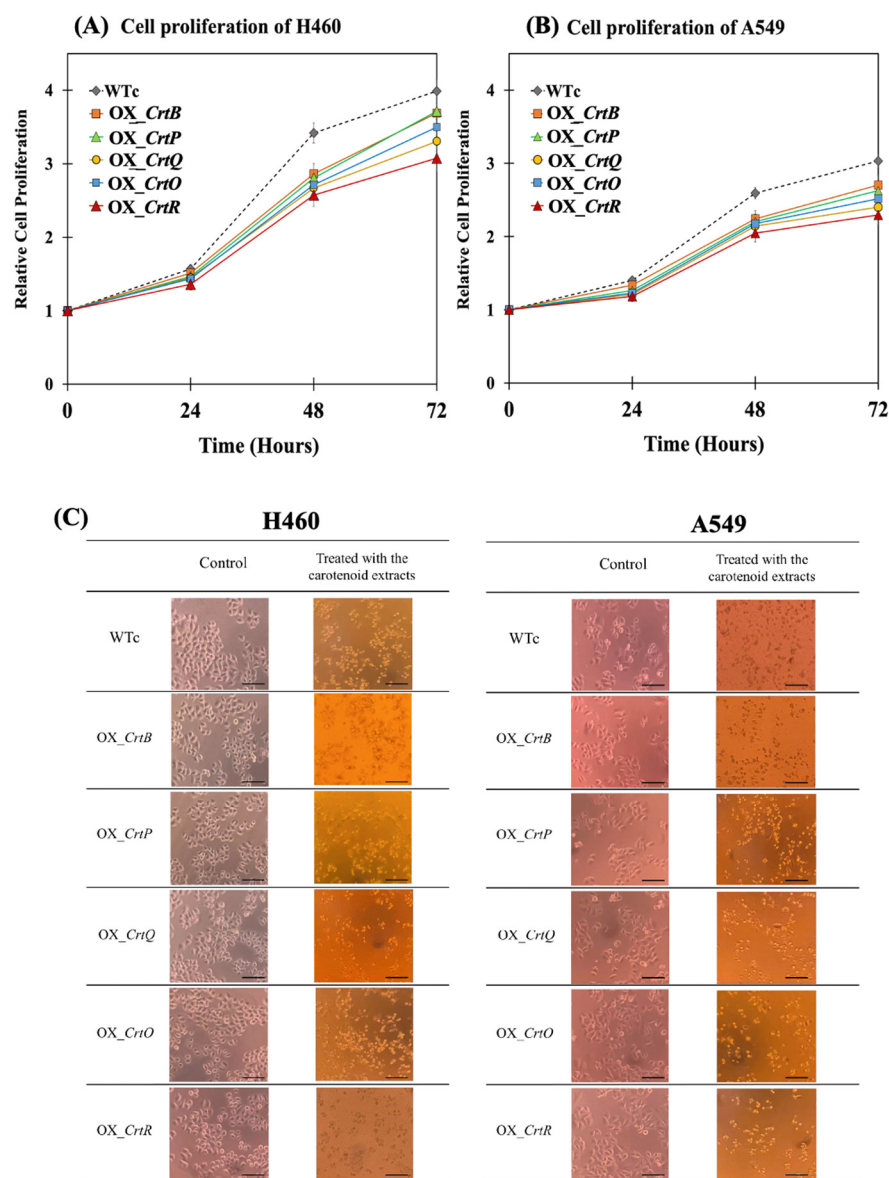


Figure 10. Cell proliferation of lung cancer cells, H460 (A) and A549 (B), and images of cell lines (C) after being treated with total carotenoids extracted from *Synechocystis* sp. PCC6803 WTc and engineered strains. For (A,B), the cancer cell lines were treated with carotenoid extracts (12.5 $\mu\text{g/mL}$) for 0, 24, 48, and 72 h at 37 $^{\circ}\text{C}$. For (C), the cancer cell lines were treated with carotenoid extracts (400 $\mu\text{g/mL}$) for 24 h at 37 $^{\circ}\text{C}$, and visualized under light microscope with a magnification of 100 \times , and a scale bar of 50 μm . Total carotenoids were extracted from cells grown in a BG₁₁ medium under high light conditions for 12 days. The error bars represent the standard deviations of means (mean \pm S.D., n = 3).

3. Discussion

In this study, we found promising results of increased carotenoid (Car) production in the cyanobacterium *Synechocystis* sp. PCC 6803 overexpressing native genes involved in Car biosynthesis with higher antioxidant activity (Figure 1). Five engineered strains, i.e., OX_CrtB, OX_CrtP, OX_CrtQ, OX_CrtO, and OX_CrtR, significantly promoted Car accumulation and altered Car-type components, particularly zeaxanthin and echinenone, except for OX_CrtQ, which also accumulated the increased β -carotene (Figures 3 and 7). All *Synechocystis* cells mostly contained the highest content of myxoxanthophyll due to its vital roles for cell wall structure and thylakoid membrane stabilization [29]. Zeaxanthin can be produced by *Synechocystis* sp. PCC 6803, while other cyanobacteria, such as *Anabaena* sp.

PCC 7120 and *Nostoc punctiforme* PCC 73102, are able to generate canthaxanthin and astaxanthin from β -carotene [30–32]. We demonstrated that a certain increase in total carotenoid accumulation in all OX strains was found during the late-log phase of cell growth, especially under light stress (Figures 3 and 6). At day 12 of normal cultivation, the native gene overexpression of *slr0088*, encoding CrtO, led to a 1.6-fold increase in echinenone, while an overexpression of *sll1468*, encoding CrtR, contained a 1.6-fold increase in zeaxanthin in comparison with the WT control (Figure 3). In a previous report, a native overexpression of CrtR in *Synechocystis* sp. PCC 6803 could induce zeaxanthin with a 2.5-fold increase compared to that in the WT strain [23]. However, we also demonstrated that a higher amount of 3'-hydroxyechinenone, in comparison with WTc, was found in both OX_CrtO and OX_CrtR strains (Figure 3). In particular, the highest level of 3'-hydroxyechinenone was induced by HL stress in OX_CrtR. When cells are exposed to intense light, the photoprotective mechanism at the phycobilisome is induced by the orange carotenoid protein (OCP)-binding hydroxyechinenone [24,33]. The high light intensity stress in this study at 150 $\mu\text{mole photon/m}^2/\text{s}$ was considered a mild photoinhibition inducer, as evidenced by the higher growth and pigment accumulation in Figures 4 and 5. *Synechocystis* cells only experienced severe photoinhibition above 800 $\mu\text{mole photon/m}^2/\text{s}$, and they displayed an efficient capacity to recover from the complete state of photoinhibition at 1460 $\mu\text{mole photon/m}^2/\text{s}$ when light exposure was reduced to 200 $\mu\text{mole photon/m}^2/\text{s}$ [34]. In addition to the higher accumulation of Cars, we also showed how the types of Cars were distributed differently. In *Synechocystis* wild-type control (Figure 7), the major Car components were myxoxanthophyll (35.3%), β -carotene (26.8%), echinenone (16%), zeaxanthin (13.2%), other minor Cars, such as 3'-hydroxyechinenone (1.5%), lycopene (0.02%), and unidentified carotenoids (7.2%). Mostly, high Cars-producing strains had lowered main components of myxoxanthophyll and β -carotene but increased zeaxanthin, 3-hydroxyechinenone, and echinenone compositions. In addition, after exposure to high light conditions in this study, WT control cells were rearranged for each Car type by inducing proportions of zeaxanthin (from 13.2% to 14.6%), 3'-hydroxyechinenone (from 1.5% to 1.6%), and β -carotene (from 26.8% to 29%), while low light conditions were handled with increased proportions of zeaxanthin (from 13.2% to 15.8%), 3'-hydroxyechinenone (from 1.5% to 2.5%), and echinenone (from 16% to 17.9%) (Figure 7). These findings suggest that zeaxanthin and 3'-hydroxyechinenone are the main Car components that respond to light stress. Zeaxanthin was previously found to enhance high light acclimation by acting as an antioxidant and lipid stabilizer in *Arabidopsis* [35]. High light stress substantially induced the binding of zeaxanthin to specific proteins in photosystems, which enhanced photoprotection and modulated chlorophyll triplet yield [5,36,37]. Both zeaxanthin and echinenone certainly modify photosystem I trimer structure and protect photosystem II repair from singlet oxygen damage in *Synechocystis* sp. PCC6803 [38–40]. It was considerably confirmed by our results that OX_CrtR with a high zeaxanthin component had the highest capacity for DPPH scavenging activity among all the strains studied (Figure 7D). Additionally, it is worth noting that increased β -carotene composition also helped wild-type cells to cope with high light stress, whereas higher echinenone composition enabled cells to handle low light stress. The native overexpression of CrtQ or *slr0940* significantly increased the highest levels of β -carotene and antioxidant activity (Figures 6 and 7). β -carotene accumulation was light-dependently induced, contributing to the acclimation to light stress in *Euglena gracilis* [41]. On the other hand, the transcript results indicated that light stress had a close relationship with enhanced carotenoid synthesis rather than degradation and chlorophyll metabolism, particularly under high light conditions (Figure 8).

We also demonstrated that carotenoid synthetic gene overexpression could improve intracellular lipid contents (Supplementary Information Figure S1). An increase in the light intensity during cultivation resulted in an increase in lipids and fatty acid production, regulating membrane integrity [42–44]. The cooperative function of lipids and carotenoids led cells to acclimate their membrane structure and function against light stress [1,28,45,46]. On the other hand, the carotenoid extracts from all engineered strains were applied to

treat lung cancer cell lines H460 and A549. Lung cancer has been the first and foremost leading cause of death around the world. A higher intake of carotenoids could lower the risk of lung cancer [17,47,48]. Our findings demonstrated that the carotenoid extracts from all engineered *Synechocystis* sp. PCC 6803 strains significantly decreased the viability and proliferation of lung cancer cell lines, particularly OX_CrtR and OX_CrtQ (Figures 9 and 10). *Synechocystis* sp. PCC 6803 overexpressing CrtR with high antioxidant activity showed the lowest level of IC₅₀ at 100.17 and 90.32 µg/mL on H460 and A549 cell lines, respectively. The anti-cancer therapeutic targets of Cars include cell cycle arrest, an apoptosis-inducing effect, an anti-metastatic effect, and an anti-angiogenic effect in cancer cells [17], as well as modulating oxidative stress and redox balance [16]. For all Car types, they have synergistic functions of antioxidant activity to modulate ROS levels and have also shown pro-oxidant effects in cancer cells [16,49]. β-carotene and lycopene were also considered potential anti-cancer compounds previously found to inhibit tumor cell growth by interfering at different phases of the cell cycle and generate apoptosis-inducing effects in cancer cells, such as the G1 phase arrest of human promyelocytic leukemia (HL-60) cells and the G0/G1 phase arrest of HL-60 cells, respectively [50,51]. In addition, β-carotene played an effective anti-metastatic role in lung cancer cells B16F-10 by reducing collagen, hydroxylproline, uronic acid, and hexamine contents [52]. On the other hand, zeaxanthin treated uveal melanoma cell lines by inducing apoptosis by activating the intrinsic apoptosis signaling pathway [53]. In accordance with our findings, *Synechocystis* sp. PCC6803 strains with CrtR and CrtQ overexpression, respectively, had the highest amounts of zeaxanthin and β-carotene. These two OX strains exhibited a certain increase in antioxidant activity, and their carotenoid extracts had the highest capacity to treat lung cancer cells in vitro.

4. Materials and Methods

4.1. Strains and Culture Conditions

Cyanobacterium *Synechocystis* sp. PCC 6803 wild-type (WT) strains and all engineered strains (Table 1) were grown in the BG₁₁ medium. The growth condition was performed at 27–30 °C under continuous white light illumination with various light intensities, including low light (LL; 10 µmole photon/m²/s), normal light (NL; 50 µmole photon/m²/s) and high light (HL; 150 µmole photon/m²/s) conditions. The cell culture flask with an initial optical density (OD) of about 0.1 at 730 nm was placed on a rotary shaker (160 rpm) for 14 days. Cell growth was spectrophotometrically measured at OD₇₃₀. The host propagation, *Escherichia coli* DH5α strain, was grown either on a Luria–Bertani (LB) agar plate or its liquid medium at 37 °C.

4.2. Constructions of Recombinant Plasmids

The recombinant plasmids (Table 1), including pEERM_CrtB, pEERM_CrtP, pEERM_CrtQ, pEERM_CrtO, and pEERM_CrtR, were constructed to generate OX_CrtB, OX_CrtP, OX_CrtQ, OX_CrtO, and OX_CrtR strains, respectively. Initially, five target gene fragments involved in the carotenoid biosynthetic pathway were amplified by PCR using each specific pair of primers, as listed in Supplementary Information Table S1, and genomic DNA as a template. Each gene fragment was then ligated into the pEERM vector with the *psbA2* promoter, which could practically let the engineered cells grow under high light conditions [54], generating the expected five recombinant plasmids listed in Table 1. pEERM_CrtB was generated via the ligation of the CrtB gene fragment amplified by FW_CrtB and RV_CrtB (Supplementary Information Table S1) with the pEERM vector in the *Pst*I restriction site. For pEERM_CrtP and pEERM_CrtQ, the CrtP and CrtQ gene fragments, amplified by a pair of FW_CrtP and RV_CrtP primers and another pair of FW_CrtQ and RV_CrtQ (Supplementary Information Table S1), respectively, were separately introduced in between *Xba*I and *Spe*I restriction sites in the pEERM vector. Moreover, pEERM_CrtO and pEERM_CrtR were generated by ligating CrtO and CrtE gene fragments, amplified by PCR using a pair of FW_CrtO and RV_CrtO and another pair of FW_CrtR and RV_CrtR

primers, respectively (Supplementary Information Table S1), in between *SpeI* and *PstI* sites in the pEERM vector.

4.3. Natural Transformation of *Synechocystis* sp. PCC 6803 Cells

The recombinant plasmids (Table 1) were transformed into *Synechocystis* sp. PCC 6803 WT cells by natural transformation, thereby generating OX_CrtB, OX_CrtP, OX_CrtQ, OX_CrtO, and OX_CrtR. To construct *Synechocystis* WT control (WTc) or *Synechocystis* WT containing the *Cm^R* cassette gene, the empty pEERM vector was transformed into *Synechocystis* WT cells. First, the host cell suspension was prepared. Then, 50 mL of *Synechocystis* sp. PCC 6803 WT cell culture with an OD₇₃₀ of about 0.5 was harvested via centrifugation at 5500 rpm (2870 × g) for 15 min. Cell pellets were resuspended in a fresh BG₁₁ medium (500 µL). After that, at least 10 µL of the recombinant plasmids were mixed with the *Synechocystis* host cell suspension and incubated in the culture room overnight. Then, the sample mixture was spread on a BG₁₁ agar plate containing 10 µg/mL of chloramphenicol. After several weeks, the colonies that survived on antibiotic plates were picked and streaked on a new BG₁₁ agar plate containing 20, and later 30 µg/mL, of chloramphenicol. The obtained transformants were confirmed for gene size, location, and segregation by PCR using many specific pairs of primers, as shown in the Supplementary Information Table S1.

4.4. Determinations of Chlorophyll *a* and Total Carotenoid Contents

The chlorophyll *a* and total carotenoid contents were analyzed using the modified method from [55]. Next, 1 mL of cell culture was extracted using the acetone:water mixture (4:1) as a solvent and incubated for 2 min. After centrifugation at 5500 rpm (2870 × g) for 5 min, the supernatant was spectrophotometrically measured at wavelengths of 470.0, 646.6, and 663.6 nm, respectively. Contents of chlorophyll *a* and carotenoids were calculated using the following equations:

$$\text{Chlorophyll } a \text{ content } (\mu\text{g}/\text{OD}_{730}) = [(12.25 \times A_{663.6}) - (2.25 \times A_{646.6})]/\text{OD}_{730}$$

$$\text{Chlorophyll } b \text{ content } (\mu\text{g}/\text{OD}_{730}) = [(20.31 \times A_{646.6}) - (4.91 \times A_{663.6})]/\text{OD}_{730}$$

$$\text{Total carotenoid content } (\mu\text{g}/\text{OD}_{730}) = [1000A_{470} - (2.27 \times \text{Chlorophyll } a \text{ content}) - (81.4 \times \text{Chlorophyll } b \text{ content})]/227 \times \text{OD}_{730}$$

4.5. Quantitative Analysis of Carotenoids by HPLC

Then, 50 mL of *Synechocystis* cell culture was harvested by centrifugation at 5500 rpm (2870 × g) for 10 min. Before starting solvent extraction, the cell suspension of all samples was diluted to an OD₇₃₀ of about 0.5. Then, cell pellets from 3 mL of diluted cell suspension were collected after centrifugation again. The intracellular pigments were then extracted by absolute methanol (1 mL), and centrifuged at 12,000 rpm (21,009 × g) and 4 °C for 5 min. After that, the supernatant was collected for further analysis. Samples of extracted intracellular pigments were detected using high-performance liquid chromatography (HPLC) (Shimadzu HPLC LGE System, Kyoto, Japan) using a C18 column, 150 × 46 mm (GL-Sciences, Tokyo, Japan). The HPLC condition was set at 15 °C, with a flow rate of 1 mL/min using the solvent system described by [1]. This solvent system consisted of an isocratic elution with a mixture of solvent A, acetonitrile: methanol: Tris (0.1 M, pH 8.0) (89/9.5/1.5, v/v), for 4 min; a linear gradient from solvent A to solvent B, methanol: hexane (4:1, v/v), for 2.5 min; an isocratic elution with solvent B for 11.5 min; a linear gradient of solvent B to solvent A for 1 min; and a final isocratic elution with solvent A for 9 min. The separated pigments were detected at 440 nm using a UV/VIS detector. The carotenoid contents, including myxoxanthophyll, zeaxanthin, 3'-hydroxy echinenone, echinenone, and β-carotene, were calculated using the following equations from [23]: $C_{\text{car}} = C_{\text{chl}} \times [(\epsilon_{\text{chl}} \times A_{\text{car}})/(\epsilon_{\text{car}} \times A_{\text{chl}})]$, where C_{chl} = the chlorophyll concentration in the pigments extracts was determined by the extinction coefficient of chlorophyll *a* using 820, and the absorbance of the pigment extract at 663 nm. ϵ_{chl} and ϵ_{car} = the specific extinction coefficients of the chlorophyll *a* and the carotenoids

at 440 nm, respectively, were taken from [56,57]. A_{chl} and A_{car} = the chlorophyll *a* and the carotenoid peak areas on the chromatogram, respectively, were detected at 440 nm. The relative amount of each carotenoid type was calculated as a percentage to the total carotenoid content under each light condition.

4.6. Determination of Lycopene Content

Lycopene content was determined using the modified method from [58]. Then, 1 mL of cell culture was extracted using the acetone:hexane solvent mixture (2:3) and incubated at room temperature for 2 min. After that, the supernatant, obtained after centrifugation at 5500 rpm ($2870 \times g$) for 10 min, was spectrophotometrically measured at four wavelengths of 453, 505, 645, and 663 nm, respectively. Lycopene content was calculated using the following equation: Lycopene content ($\mu\text{g}/\text{OD}_{730}$) = $[(-0.0485 \times A_{663}) + (0.204 \times A_{645}) + (0.372 \times A_{505}) - (0.0806 \times A_{453})]/100,000 \times \text{OD}_{730}$, where *A* = absorbance.

4.7. Total RNA Extraction and Reverse Transcription–Polymerase Chain Reaction (RT-PCR)

The total RNAs were extracted from all strains using the TRIzol[®] reagent (Invitrogen, Life Technologies Corporation, Carlsbad, CA, USA). The purified RNAs (1 μg) were converted to cDNA using the SuperScript III First-Strand Synthesis Kit (Invitrogen, Carlsbad, CA, USA). Then, the obtained cDNA was used as a template for PCR with various pairs of specific primers, as listed in Supplementary Information Table S1. We monitored the *CrtB*, *CrtP*, *CrtQ*, *CrtR*, and *CrtO* genes in relation to the carotenoid biosynthetic pathway; the *Diox1* gene in carotenoid degradation or retinal biosynthesis; the *ChlP* and *ChlG* genes in chlorophyll biosynthesis; and the *Slr1652* gene in chlorophyll degradation. The 16s rRNA was used as a reference. The PCR reaction mixture using KOD One[™] Master Mix (Toyobo, Osaka, Japan) and its conditions were performed by suitable cycles of each gene at 98 °C for 10 s, at both a primer melting temperature (*T_m*, Supplementary Information Table S1) for 5 s and 68 °C for 5 s. Then, the PCR products were checked by 1% (*w/v*) agarose gel electrophoresis. The quantification of band intensity was detected by Syngene[®] Gel Documentation (Syngene, Frederick, MD, USA).

4.8. Determination of DPPH Radical Scavenging Activity

The free radical scavenging activity of pigment extracts from all strains was measured using a DPPH assay (modified from [59]). Then, 1 mL of cell culture was harvested by centrifugation at 5500 rpm ($2870 \times g$) for 10 min. Pigment extracts were obtained from cell pellets after they were incubated with a solvent mixture of acetone and water (4:1) at room temperature for 10 min. The 2,2-diphenyl-1-picrylhydrazyl (DPPH) concentration was prepared as 0.1 mM in ethanol. The DPPH solution (500 μL) was mixed with the cell-free pigment extract (500 μL). The reaction mixture was incubated at room temperature for 30 min. After that, the absorbance at 517 nm was spectrophotometrically measured. An ascorbic acid was used as a standard. The antioxidant activity was calculated using the equation; DPPH radical scavenging activity (%) = $(A_0 - A_1)/A_0 \times 100$, where A_0 is the absorbance of the control reaction and A_1 is the absorbance of the sample.

4.9. Cell Line Culture

NSCLC cell lines A549 (CCL-185) and H460 (HTB-177) were obtained from the American Type Culture Collection (ATCC; Manassas, VA, USA). The H460 cell line was obtained from the pleural fluid of a male patient with large cell lung cancer, while the A549 cell line was obtained from an explant culture of lung carcinomatous tissue from an old male patient. The A549 cells were cultured in Dulbecco's modified Eagle medium (DMEM), while the H460 cells were cultured in Roswell Park Memorial Institute 1640 medium (RPMI-1640). Both media were supplemented with 10% fetal bovine serum albumin, 2 mM L-glutamine, and 100 U/mL of penicillin–streptomycin (Invitrogen, Carlsbad, CA, USA). Cell culture was maintained in a humidified atmosphere containing 5% CO₂ at 37 °C. The culture medium and trypsinization were renewed every 2–3 days. 3-(4,5-dimethylthiazol-2-yl)-2,5-

diphenyltetrazolium bromide (MTT) (Invitrogen, Carlsbad, CA, USA) solution (5 mg/mL) was freshly prepared in phosphate-buffered saline (PBS).

4.10. Cytotoxicity and Cell Proliferative Assay

Total carotenoids were extracted from all strains by a solvent mixture of hexane:acetone:ethanol (50:25:25, *v/v/v*) and a subsequent 1 M KOH solution to remove chlorophyll (modified from [60]). After the centrifugation was performed at 5500 rpm ($2870\times g$), 4 °C for 10 min, the upper fraction layer of hexane containing total carotenoid extracts was carefully collected, and the solvent was evaporated under nitrogen gas at room temperature. Extracted carotenoid powder was dissolved in a PBS buffer with 0.25% (*v/v*) dimethyl sulfoxide (DMSO; Sigma, St. Louis, MO, USA), the maximum DMSO concentration that did not interfere with the assays in various concentrations (0–400 µg/mL).

The cytotoxicity of the extracts was determined by the MTT assay (modified from [14,61]). Cell lines were seeded into 96-well plates at a density of 10,000 cells per well and incubated at 37 °C overnight for cell attachment purposes. The cells were then treated with various concentrations of carotenoid extracts ranging from 0 to 400 µg/mL for 24 h. After the incubation period of 24 h, 10 µL of MTT solution (5 mg/mL) was added to each well and incubated at 37 °C for 4 h. After the incubation period, the resulting formazan crystals were formed, and dissolved in 100 µL of DMSO. After that, the colored product was spectrophotometrically measured at 570 nm. The results from the MTT assay represented the IC₅₀ value of the different carotenoid extracts from all strains by analyzing their effect on cell viability.

Cell proliferative assay was determined by the MTT assay (modified from [62]). Cell lines were seeded at a density of 3000 cells per well into 96-well plates. Cells were treated with non-toxic concentrations of the carotenoid extracts (12.5 µg/mL) and incubated at 37 °C for 24, 48, and 72 h. After the incubation at each elapsed time, 10 µL of MTT (5 mg/mL) was added into each well and incubated at 37 °C for 4 h. The formazan crystals were formed and later dissolved by 100 µL of DMSO. After that, the sample was spectrophotometrically measured at 570 nm. Relative cell proliferation was calculated by dividing the OD₅₇₀ of the treated group by the OD₅₇₀ of the control.

4.11. Statistical Analysis

Statistical analyses were performed using SPSS version 29.0, licensed by Chulalongkorn University. The differences in biochemical parameters and molecular responses among the treatments were analyzed using one-way ANOVA, followed by Tukey's HSD test for the multiple comparison tests. The *t*-test was performed for an independent two-pair comparison test. Non-parametric tests were used for the data which did not meet the assumption of normality. The significant differences were accepted at $p < 0.05$.

5. Conclusions

Five engineered *Synechocystis* sp. PCC 6803 strains with high carotenoid accumulation and antioxidant activity were achieved by overexpressing five carotenoid biosynthetic genes, thereby generating OX_CrtB, OX_CrtP, OX_CrtQ, OX_CrtO, and OX_CrtR. The increased levels of zeaxanthin and echinenone were mostly found in all engineered strains, whereas myxoxanthophyll was maintained as the main carotenoid type. An increase in carotenoid content was especially induced under high light stress at 150 µmole photon/m²/s, except for β-carotene. Changes in the components of all carotenoid types were considered a marker that responded to light stress. Additionally, all modified strains were more susceptible to high light-stress-induced lipid accumulation. It is worth noting that the extracted carotenoids with high antioxidant activity from all engineered strains efficiently treated lung cancer cells H460 and A549 by decreasing their cell viability and proliferation, particularly OX_CrtR and OX_CrtQ, with high levels of zeaxanthin and β-carotene, respectively. Although the mechanisms of all carotenoid types treating cancer cells are still not completely elucidated, this study highlights a promising step towards the cyanobacte-

rial application on health and cancer treatment aspects from renewable biosources. It would be useful to characterize and gain more understanding about carotenoid mechanisms or perform animal model testing on the carotenoid extracts in vivo.

Supplementary Materials: The supporting information can be downloaded at: <https://www.mdpi.com/article/10.3390/ijms24119370/s1>.

Author Contributions: Conceptualization, S.J., V.P. and P.L.; methodology, S.J.; validation, S.J. and V.P.; formal analysis, M.N.; investigation, M.N.; resources, S.J.; data curation, S.J. and M.N.; writing—original draft preparation, M.N. and S.J.; writing—review and editing, S.J.; visualization, M.N. and S.J.; supervision, S.J. and V.P.; project administration, S.J.; funding acquisition, M.N. and S.J. All authors have read and agreed to the published version of the manuscript.

Funding: This research was funded by grants from the 100th Anniversary Chulalongkorn University Fund for Doctoral Scholarship, and a partial research funding from the Graduate School, Chulalongkorn University to M.N., and the 90th Anniversary of Chulalongkorn University Fund (Ratchadaphiseksomphot Endowment Fund) to M.N. and S.J.

Institutional Review Board Statement: Not applicable.

Informed Consent Statement: Not applicable.

Data Availability Statement: Not applicable.

Conflicts of Interest: The authors declare no conflict of interest.

Abbreviations

Cars	carotenoids
Cm	chloramphenicol
DMEM	Dulbecco's modified Eagle medium
DMSO	dimethyl sulfoxide
DPPH	2,2-diphenyl-1-picrylhydrazyl
h	hour
kb	kilobase
LB medium	Luria–Bertani medium
m	meter
M	molar
mM	millimolar
mg	milligram
mL	milliliter
min	minutes
µg	microgram
µL	microliter
nm	nanometer
MTT	3-(4,5-dimethylthiazol-2-yl)-2,5-diphenyltetrazolium bromide
OCP	orange carotenoid protein
OD	optical density
OX strain	overexpressed strain
PCR	polymerase chain reaction
ROS	reactive oxygen species
Rpm	revolutions per minute
RPMI-1640	Roswell Park Memorial Institute 1640
s	second
WT	wild type

References

1. Zhang, L.; Selão, T.T.; Selstam, E.; Norling, B. Subcellular localization of carotenoid biosynthesis in *Synechocystis* sp. PCC 6803. *PLoS ONE* **2015**, *10*, e0130904. [[CrossRef](#)] [[PubMed](#)]
2. Gruszecki, W.I.; Strzałka, K. Carotenoids as modulators of lipid membrane physical properties. *Biochem. Biophys. Acta—Mol. Basis Dis.* **2005**, *1740*, 108–115. [[CrossRef](#)] [[PubMed](#)]

3. Tóth, T.N.; Chukhutsina, V.; Domonkos, I.; Knoppová, J.; Komenda, J.; Kis, M.; Lénárt, Z.; Garab, G.; Kovács, L.; Gombos, Z.; et al. Carotenoids are essential for the assembly of cyanobacterial photosynthetic complexes. *Biochim. Biophys. Acta* **2015**, *1847*, 1153–1165. [[CrossRef](#)] [[PubMed](#)]
4. Santabarbara, S.; Casazza, A.P.; Ali, K.; Economou, C.K.; Wannathong, T.; Zito, F.; Redding, K.E.; Rappaport, F.; Purton, S. The requirement for carotenoids in the assembly and function of the photosynthetic complexes in *Chlamydomonas reinhardtii*. *Plant Physiol.* **2013**, *161*, 535–546. [[CrossRef](#)] [[PubMed](#)]
5. Zakar, T.; Laczko-Dobos, H.; Tóth, T.N.; Gombos, Z. Carotenoids assist in cyanobacterial photosystem II assembly and function. *Front. Plant Sci.* **2016**, *7*, 295. [[CrossRef](#)]
6. Croce, R.; van Amerongen, H. Natural strategies for photosynthetic light harvesting. *Nat. Chem. Biol.* **2014**, *10*, 492–501. [[CrossRef](#)]
7. Schäfer, L.; Sandmann, M.; Woitsch, S.; Sandmann, G. Coordinate up-regulation of carotenoid biosynthesis as a response to light stress in *Synechococcus* PCC7942. *Plant Cell Environ.* **2006**, *29*, 1349–1356. [[CrossRef](#)]
8. Ehling-Schulz, M.; Bilger, W.; Scherer, S. UV-B-induced synthesis of photoprotective pigments and extracellular polysaccharides in the terrestrial cyanobacterium *Nostoc commune*. *J. Bacteriol.* **1997**, *179*, 1940–1945. [[CrossRef](#)]
9. Packer, J.E.; Mahood, J.S.; Mora-Arellano, V.O.; Slater, T.F.; Willson, R.L.; Wolfenden, B.S. Free radicals and singlet oxygen scavengers: Reaction of a peroxy-radical with beta-carotene, diphenylfuran and 1,4-diazobicyclo (2,2,2)-octane. *Biochem. Biophys. Res. Commun.* **1981**, *98*, 901–906. [[CrossRef](#)]
10. Stratton, S.P.; Schaefer, W.H.; Liebler, D.C. Isolation and identification of singlet oxygen oxidation products of beta-carotene. *Chem. Res. Toxicol.* **1993**, *6*, 542–547. [[CrossRef](#)]
11. Ramel, F.; Birtic, S.; Cuiné, S.; Triantaphylidès, C.; Ravanat, J.L.; Michel Havaux, M. Chemical quenching of singlet oxygen by carotenoids in plants. *Plant Physiol.* **2012**, *158*, 1267–1278. [[CrossRef](#)]
12. Domonkos, I.; Mihály Kis, M.; Gombos, Z.; Ughy, B. Carotenoids, versatile components of oxygenic photosynthesis. *Prog. Lipid Res.* **2013**, *52*, 539–561. [[CrossRef](#)] [[PubMed](#)]
13. Krinsky, N.I.; Johnson, E.J. Carotenoid actions and their relation to health and disease. *Mol. Aspects Med.* **2005**, *26*, 459–516. [[CrossRef](#)] [[PubMed](#)]
14. Lopes, G.; Clarinha, D.; Vasconcelos, V. Carotenoids from cyanobacteria: A biotechnological approach for the topical treatment of psoriasis. *Microorganisms* **2020**, *8*, 302. [[CrossRef](#)] [[PubMed](#)]
15. Nandagopal, P.; Steven, A.N.; Chan, L.W.; Rahmat, Z.; Jamaluddin, H.; Mohd Noh, N.I. Bioactive metabolites produced by cyanobacteria for growth adaptation and their pharmacological properties. *Biology* **2021**, *10*, 1061. [[CrossRef](#)]
16. Saini, R.K.; Keum, Y.S.; Daglia, M.; Rengasamy, K.R.R. Dietary carotenoids in cancer chemoprevention and chemotherapy: A review of emerging evidence. *Pharmacol. Res.* **2020**, *157*, 104830. [[CrossRef](#)] [[PubMed](#)]
17. Niranjana, R.; Gayathri, R.; Nimish Mol, S.; Sugawara, T.; Hirata, T.; Miyashita, K.; Ganesan, P. Carotenoids modulate the hallmarks of cancer cells. *J. Funct. Foods* **2015**, *18*, 968–985. [[CrossRef](#)]
18. Arathi, B.P.; Sowmya, P.R.R.; Kuriakose, G.C.; Vijay, K.; Baskaran, V.; Jayabaskaran, C.; Lakshminarayana, R. Enhanced cytotoxic and apoptosis inducing activity of lycopene oxidation products in different cancer cell lines. *Food Chem. Toxicol.* **2016**, *97*, 265–276. [[CrossRef](#)]
19. Jomova, K.; Valko, M. Health protective effects of carotenoids and their interactions with other biological antioxidants. *Eur. J. Med. Chem.* **2013**, *70*, 102–110. [[CrossRef](#)]
20. Firczuk, M.; Bajor, M.; Graczyk-Jarzynka, A.; Fidy, K.; Goral, A.; Zagodzón, R. Harnessing altered oxidative metabolism in cancer by augmented prooxidant therapy. *Cancer Lett.* **2020**, *471*, 1–11. [[CrossRef](#)]
21. Maresca, J.A.; Graham, J.E.; Wu, M.; Eisen, J.A.; Bryant, D.A. Identification of a fourth family of lycopene cyclases in photosynthetic bacteria. *Proc. Natl. Acad. Sci. USA* **2007**, *104*, 11784–11789. [[CrossRef](#)] [[PubMed](#)]
22. Mohamed, H.E.; Vermaas, W.F.J. S110254 (CrtL(diox)) is a bifunctional lycopene cyclase/dioxygenase in cyanobacteria producing myxoxanthophyll. *J. Bacteriol.* **2006**, *188*, 3337–3344. [[CrossRef](#)] [[PubMed](#)]
23. Lagarde, D.; Vermaas, W. The zeaxanthin biosynthesis enzyme beta-carotene hydroxylase is involved in myxoxanthophyll synthesis in *Synechocystis* sp. PCC6803. *FEBS Lett.* **1999**, *454*, 247–251.
24. Punginelli, C.; Wilson, A.; Routaboul, J.M.; Kirilovsky, D. Influence of zeaxanthin and echinenone binding on the activity of the orange carotenoid protein. *Biochim. Biophys. Acta* **2009**, *1787*, 280–288. [[CrossRef](#)]
25. Vavilin, D.; Vermass, W. Continuous chlorophyll degradation accompanied by chlorophyllide and phytol reutilization for chlorophyll synthesis in *Synechocystis* sp. PCC 6803. *Biochim. Biophys. Acta Bioenerg.* **2007**, *1767*, 920–929. [[CrossRef](#)] [[PubMed](#)]
26. Walter, M.H.; Strack, D. Carotenoids and their cleavage products: Biosynthesis and functions. *Nat. Prod. Rep.* **2011**, *28*, 663. [[CrossRef](#)] [[PubMed](#)]
27. Chen, Q.; van der Steen, J.B.; Arents, J.C.; Hartog, A.F.; Ganapathy, S.; de Grip, W.J.; Hellingwerf, K.J. Deletion of *sl11541* in *Synechocystis* sp. strain PCC 6803 allows formation of a far-red-shifted holoproteorhodopsin in vivo. *Appl. Environ. Microbiol.* **2018**, *84*, e02435-17. [[CrossRef](#)] [[PubMed](#)]
28. Zakar, T.; Herman, E.; Vajravel, S.; Kovacs, L.; Knoppová, J.; Komenda, J.; Domonkos, I.; Kis, M.; Gombos, Z.; Laczko-Dobos, H. Lipid and carotenoid cooperation-driven adaptation to light and temperature stress in *Synechocystis* sp. PCC6803. *Biochim. Biophys. Acta Bioenerg.* **2017**, *1858*, 337–350. [[CrossRef](#)]

29. Mohamed, H.E.; van de Meene, A.M.L.; Roberson, R.W.; Vermaas, W.F.J. Myxoxanthophyll is required for normal cell wall structure and thylakoid organization in the cyanobacterium *Synechocystis* sp. strain PCC 6803. *J. Bacteriol.* **2005**, *187*, 6883–6892. [\[CrossRef\]](#)
30. Makino, T.; Harada, H.; Ikenaga, H.; Matsuda, S.; Takaichi, S.; Shindo, K.; Sandmann, G.; Ogata, T.; Misawa, N. Characterization of cyanobacterial carotenoid ketolase CrtW and hydroxylase CrtR by complementation analysis in *Escherichia coli*. *Plant Cell Physiol.* **2008**, *49*, 1867–1878. [\[CrossRef\]](#)
31. Takaichi, S.; Maoka, T.; Masamoto, K. Myxoxanthophyll in *Synechocystis* sp. PCC 6803 is myxol 2'-dimethyl-fucoside, (3R,2'S)-myxol 2'-(2,4-di-O-methyl- α -L-fucoside), not rhamnoside. *Plant Cell Physiol.* **2001**, *42*, 756–762. [\[CrossRef\]](#) [\[PubMed\]](#)
32. Takaichi, S. Carotenoids in algae: Distributions, biosyntheses and functions. *Mar. Drugs* **2011**, *9*, 1101–1118. [\[CrossRef\]](#) [\[PubMed\]](#)
33. Polívka, T.; Chábera, P.; Kerfeld, C.A. Carotenoid–protein interaction alters the S1 energy of hydroxyechinenone in the Orange Carotenoid Protein. *Biochim. Biophys. Acta* **2013**, *1827*, 248–254. [\[CrossRef\]](#) [\[PubMed\]](#)
34. Condara, A.; Re, A.; Pagliano, C.; Van Alphen, P.; Pirone, R.; Saracco, G.; Branco Dos Santos, F.; Hellingwerf, K.; Vasile, N. Analysis of the light intensity dependence of the growth of *Synechocystis* and of the light distribution in a photobioreactor energized by 635 nm light. *PeerJ* **2018**, *6*, e5256. [\[CrossRef\]](#) [\[PubMed\]](#)
35. Müller-Moulé, P.; Havaux, M.; Niyogi, K.K. Zeaxanthin deficiency enhances the high light sensitivity of an ascorbate-deficient mutant of *Arabidopsis*. *Plant Physiol.* **2003**, *133*, 748–760. [\[CrossRef\]](#)
36. Dall'Osto, L.; Holt, N.E.; Kaligotla, S.; Fuciman, M.; Cazzaniga, S.; Carbonera, D.; Frank, H.A.; Alric, J.; Bassi, R. Zeaxanthin protects plant photosynthesis by modulating chlorophyll triplet yield in specific light-harvesting antenna subunits. *J. Biol. Chem.* **2012**, *287*, 41820–41834. [\[CrossRef\]](#) [\[PubMed\]](#)
37. Ballottari, M.; Alcocer, M.J.P.; D'Andrea, C.; Viola, D.; Ahn, T.K.; Petrozza, A.; Polli, D.; Fleming, G.R.; Cerullo, G.; Bassi, R. Regulation of photosystem I light harvesting by zeaxanthin. *Proc. Natl. Acad. Sci. USA* **2014**, *111*, E2431–E2438. [\[CrossRef\]](#)
38. Vajravel, S.; Kis, M.; Kłodawska, K.; Laczko-Dobos, H.; Malec, P.; Kovács, L.; Gombos, Z.; Toth, T.N. Zeaxanthin and echinenone modify the structure of photosystem I trimer in *Synechocystis* sp. PCC 6803. *Biochim. Biophys. Acta Bioenerg.* **2017**, *1858*, 510–518. [\[CrossRef\]](#)
39. Kusama, Y.; Inoue, S.; Jimbo, H.; Takaichi, S.; Sonoike, K.; Hihara, Y.; Nishiyama, Y. Zeaxanthin and echinenone protect the repair of photosystem II from inhibition by singlet oxygen in *Synechocystis* sp. PCC 6803. *Plant Cell Physiol.* **2015**, *56*, 906–916. [\[CrossRef\]](#)
40. Isukara, T.; Kaihatsu, I.; Jimbo, H.; Takaichi, S.; Nishiyama, Y. Elevated levels of specific carotenoids during acclimation to strong light protect the repair of photosystem II in *Synechocystis* sp. PCC 6803. *Front. Plant Sci.* **2020**, *11*, 1030.
41. Tanno, Y.; Kato, S.; Takahashi, S.; Tamaki, S.; Takaichi, S.; Kodama, Y.; Sonoike, K.; Shinomura, T. Light dependent accumulation of β -carotene enhances photoacclimation of *Euglena gracilis*. *J. Photochem. Photobiol. Biol.* **2020**, *209*, 111950. [\[CrossRef\]](#) [\[PubMed\]](#)
42. Hempel, N.; Petrick, I.; Behrrendt, F. Biomass productivity and productivity of fatty acids and amino acids of microalgae strains as key characteristics of suitability for biodiesel production. *J. Appl. Phycol.* **2012**, *24*, 1407–1418. [\[CrossRef\]](#) [\[PubMed\]](#)
43. Takeshita, T.; Ota, S.; Yamazaki, T.; Hirata, A.; Zachleder, V.; Kawano, S. Starch and lipid accumulation in eight strains of six *Chlorella* species under comparatively high light intensity and aeration culture conditions. *Bioresour. Technol.* **2014**, *158*, 127–134. [\[CrossRef\]](#) [\[PubMed\]](#)
44. Maltsev, Y.; Maltseva, K.; Kulikovskiy, M.; Maltseva, S. Influence of light conditions on microalgae growth and content of lipids, carotenoids, and fatty acid composition. *Biology* **2021**, *10*, 1060. [\[CrossRef\]](#)
45. Kim, S.-H.; Liu, K.-H.; Lee, S.-Y.; Hong, S.-J.; Cho, B.-K.; Lee, H.; Lee, C.-G.; Choi, H.-K. Effects of light intensity and nitrogen starvation on glycerolipid, glycerophospholipid, and carotenoid composition in *Dunaliella tertiolecta* culture. *PLoS ONE* **2013**, *8*, e72415. [\[CrossRef\]](#)
46. Shin, J.; Song, M.-H.; Oh, J.-W.; Keum, Y.-S.; Saini, R.K. Pro-oxidant actions of carotenoids in triggering apoptosis of cancer cells: A review of emerging evidence. *Antioxidants* **2020**, *9*, 532. [\[CrossRef\]](#)
47. Holick, C.N.; Michaud, D.S.; Stolzenberg-Solomon, R.; Mayne, S.T.; Pietinen, P.; Taylor, P.R.; Virtamo, J.; Albanes, D. Dietary carotenoids, serum β -carotene, and retinol and risk of lung cancer in the α -tocopherol, β -carotene cohort study. *Am. J. Epidemiol.* **2002**, *156*, 536–547. [\[CrossRef\]](#)
48. Takata, Y.; Xiang, Y.B.; Yang, G.; Li, H.; Gao, J.; Cai, H.; Gao, Y.T.; Zheng, W.; Shu, X.O. Intakes of fruits, vegetables, and related vitamins and lung cancer risk: Results from the Shanghai Men's Health Study (2002–2009). *Nutr. Cancer.* **2013**, *65*, 51–61. [\[CrossRef\]](#)
49. Vijay, K.; Sowmya, P.R.-R.; Arathi, B.P.; Shilpa, S.; Shwetha, H.J.; Raju, M.; Baskaran, V.; Lakshminarayana, R. Low-dose doxorubicin with carotenoids selectively alters redox status and upregulates oxidative stress-mediated apoptosis in breast cancer cells. *Food Chem. Toxicol.* **2018**, *118*, 675–690. [\[CrossRef\]](#)
50. Upadhyaya, K.R.; Radha, K.S.; Madhyastha, H.K. Cell cycle regulation and induction of apoptosis by β -carotene in U937 and HL-60 leukemia cells. *J. Biochem. Mol. Biol.* **2007**, *40*, 1009–1015. [\[CrossRef\]](#)
51. Amir, H.; Karas, M.; Giat, J.; Danilenko, M.; Levy, R.; Yermiah, T.; Levy, J.; Sharoni, Y. Lycopene and 1,25-dihydroxyvitamin D3 cooperate in the inhibition of cell cycle progression and induction of differentiation in HL-60 leukemic cells. *Nutr. Cancer* **1999**, *33*, 105–112. [\[CrossRef\]](#) [\[PubMed\]](#)
52. Pradeep, C.; Kuttan, G. Effect of β -carotene on the inhibition of lung metastasis in mice. *Phytomedicine* **2003**, *10*, 159–164. [\[CrossRef\]](#) [\[PubMed\]](#)

53. Bi, M.C.; Rosen, R.; Zha, R.Y.; McCormick, S.A.; Song, E.; Hu, D.N. Zeaxanthin induces apoptosis in human uveal melanoma cells through Bcl-2 family proteins and intrinsic apoptosis pathway. *Evid. Based Complement. Alternat. Med.* **2013**, *2013*, 205082. [[CrossRef](#)] [[PubMed](#)]
54. Englund, E.; Andersen-Ranberg, J.; Miao, R.; Hamberger, B.; Lindberg, P. Metabolic engineering of *Synechocystis* sp. PCC 6803 for production of the plant diterpenoid manoyl oxide. *ACS Synth. Biol.* **2015**, *4*, 1270–1278. [[CrossRef](#)] [[PubMed](#)]
55. Yang, C.M.; Chang, K.W.; Yin, M.H.; Huang, H.M. Methods for the determination of the chlorophylls and their derivatives. *Taiwania* **1998**, *43*, 116–122.
56. Mantoura, R.F.C.; Llewellyn, C.A. The rapid determination of algal chlorophyll and carotenoid pigments and their breakdown products in natural waters by reverse-phase high-performance liquid chromatography. *Anal. Chim. Acta* **1983**, *151*, 297–314. [[CrossRef](#)]
57. Inouye, C.Y.; Hill, G.E.; Stradi, R.D.; Montgomerie, R. Carotenoid pigments in male house finch plumage in relation to age, subspecies, and ornamental coloration. *Auk* **2001**, *118*, 900–915. [[CrossRef](#)]
58. Nagata, M.; Yamashita, I. Simple method for simultaneous determination of chlorophyll and carotenoids in tomato fruit. *Nippon Shokuhin Kogyo Gakkaishi* **1992**, *39*, 925–928. [[CrossRef](#)]
59. Hossain, M.F.; Ratnayake, R.R.; Meerajini, K.; Wasantha Kumara, K.L. Antioxidant properties in some selected cyanobacteria isolated from fresh water bodies of Sri Lanka. *Food Sci. Nutr.* **2016**, *4*, 753–758. [[CrossRef](#)]
60. Lee, H.S.; Castle, W.S. Seasonal changes of carotenoid pigments and color in Hamlin, Earlygold, and Budd Blood orange juices. *J. Agric. Food Chem.* **2001**, *49*, 877–882. [[CrossRef](#)]
61. Elkeiy, M.M.; Khamis, A.A.; El-Gamal, M.M.; Abo Gazia, M.M.; Zalat, Z.A.; El-Magd, M.A. Chitosan nanoparticles from *Artemia salina* inhibit progression of hepatocellular carcinoma in vitro and in vivo. *Environ. Sci. Pollut. Res.* **2020**, *27*, 19016–19028. [[CrossRef](#)] [[PubMed](#)]
62. Wang, W.; Chen, K.; Liu, Q.; Johnston, N.; Ma, Z.; Zhang, F.; Zheng, X. Suppression of tumor growth by *Pleurotus ferulae* ethanol extract through induction of cell apoptosis, and inhibition of cell proliferation and migration. *PLoS ONE* **2014**, *9*, e102673. [[CrossRef](#)] [[PubMed](#)]

Disclaimer/Publisher’s Note: The statements, opinions and data contained in all publications are solely those of the individual author(s) and contributor(s) and not of MDPI and/or the editor(s). MDPI and/or the editor(s) disclaim responsibility for any injury to people or property resulting from any ideas, methods, instructions or products referred to in the content.